

Monitoring of a Coastal Zone by Independent Fast Photogrammetric Surveys: the Case of Monterosso a Mare (Ligurian Sea, Italy)

Arianna Pesci^{1,*}, Giordano Teza², Marina Bisson³, Filippo Muccini⁴, Paolo Stefanelli⁴, Marco Anzidei⁵, Roberto Carluccio⁴, Iacopo Nicolosi⁴, Alessandro Galvani⁵, Vincenzo Sepe⁵, Cosmo Carmisciano⁴

¹Istituto Nazionale di Geofisica e Vulcanologia, Sezione di Bologna, via Creti 12, 40128 Bologna, Italy

²Dipartimento di Geoscienze, Università degli Studi di Padova, via Gradenigo, 6, 35131 Padova, Italy

³Istituto Nazionale di Geofisica e Vulcanologia, Sezione di Pisa, via della Faggiola, 32, 56126 Pisa, Italy

⁴Istituto Nazionale di Geofisica e Vulcanologia, Sezione di Roma2, via di Vigna Murata 605, 00143 Roma, Italy

⁵Istituto Nazionale di Geofisica e Vulcanologia, CNT, via di Vigna Murata 605, 00143 Roma, Italy

*Corresponding author: arianna.pesci@ingv.it

Abstract The Structure-from-Motion photogrammetry (SfM) allows a fast and easy data acquisition and a highly automated data processing, leading to accurate photorealistic point clouds. The results of a SfM-based modeling of the coastal zone of Monterosso a Mare (Eastern Liguria, Italy) are shown here. Four photogrammetric surveys of the area were carried out from both moving surface (boat) and aerial (Unmanned Aerial Vehicle) platforms. The corresponding results were compared in order to provide information about precision and model reliability from fast and cheap SfM surveys carried out without Ground Control Points (GCPs). The important issue of scale factor evaluation was solved by means of selection of points easily recognizable in each point cloud and measurement of the length of the polyline that connects these points. The ratio between the lengths of the polyline defined on a point cloud and the corresponding polyline defined in a metric reference frame provided the scale factor. The results highlight that the SfM technique can be used in emergency conditions, where GCPs cannot be used, and is compatible with a floating platform-based observation, leading to point clouds whose resolution is some centimeters for an acquisition distance of 100-150 m.

Keywords: photogrammetry, structure-from-motion, fast surveying, monitoring, 3D modeling, coast

Cite This Article: Arianna Pesci, Giordano Teza, Marina Bisson, Filippo Muccini, Paolo Stefanelli, Marco Anzidei, Roberto Carluccio, Iacopo Nicolosi, Alessandro Galvani, Vincenzo Sepe, and Cosmo Carmisciano, "Monitoring of a Coastal Zone by Independent Fast Photogrammetric Surveys: the Case of Monterosso a Mare (Ligurian Sea, Italy)." *Journal of Geosciences and Geomatics*, vol. 4, no. 4 (2016): 73-81. doi: 10.12691/jgg-4-4-1.

1. Introduction

The geo-morphological changes of an area affected by surface deformation, gravitative instabilities, landslide evolution, rock-falls and other surface phenomena, can be successfully revealed and quantified by high-accuracy Digital Surface Models (DSM) and Digital Terrain Models (DTM). A DSM represents the Earth's surface includes topography and all natural or human-made features on it. Instead, a DTM represents the bare ground surface without any features [1]. If a sub-vertical cliff is studied, a reference plane roughly parallel to such a cliff could be used in surface modeling. The comparison between multitemporal models provides a space-time description of the ongoing processes, useful to estimate deformation patterns, ground displacements, surface variations, volumes involved in mass movements and other physical features, also in marine environment [2]. Static, quasi-static and kinematic GNSS (Global Navigation Satellite System) measurements, airborne and

terrestrial digital photogrammetry and laser scanning, satellite-based and ground-based interferometric radar, and optical satellite imagery, are all suitable surveying methods that provide data of suitable spatial resolution (see e.g. [3,4,5]). However, most of these techniques still require expensive equipment and long processing time.

The Structure-from-Motion photogrammetry (SfM) provides high resolution and accurate three-dimensional spatial data throughout simple and cheap images acquisition. As in traditional photogrammetry, SfM employs overlapping images acquired from multiple viewpoints (VPs) but provides 3D reconstruction by automatically calculating camera position and orientation without the need for a pre-defined set of Ground Control Points (GCPs), i.e. points at known positions in the space recognized in the acquired images [6].

This paper presents a SfM-based 3D modeling of the coastal zone of Monterosso a Mare (Eastern Liguria, Italy). Results from four photogrammetric surveys carried out from sailing and aerial platforms (a boat and an Unmanned Aerial Vehicle, UAV, respectively) are shown and compared providing information about precision and

model reliability from fast and cheap SfM surveys carried out without use of GCPs. The test is conceived in order to verify if fast photogrammetric surveying is compatible with the morphological characterization of an observed surface. In particular, the test aims at verifying if the comparison between the digital model generated from a fast survey and an available reference model can highlight a deformation pattern, new features, holes and/or volumetric changes. For these reasons, a decimeter/sub-decimeter accuracy is desired.

2. Geographical and Geological Setting

The investigated area is the bay of Monterosso (Municipality of Monterosso a Mare, La Spezia, Italy), one of the villages of Cinque Terre (Figure 1a), belonging to the National Park delle Cinque Terre [7]. The coastal landscape mainly consists of steep rocky slopes shaped by the sea erosion in the basal portion and by hydro-geological processes and human activity (terraced landscaped related to the agricultural activities) in the upper part. The geologic setting of this area (Figure 1b, Figure 1c) is a consequence of the tectonic phases related to the opening, evolution and closure of the Ligurian-Piedmont oceanic basin ([8,9,10]). This sector of the Eastern Liguria Apennines experienced Quaternary surface uplift at 1 mm/yr [11] with subsequent formation of unstable marine terraces [12].

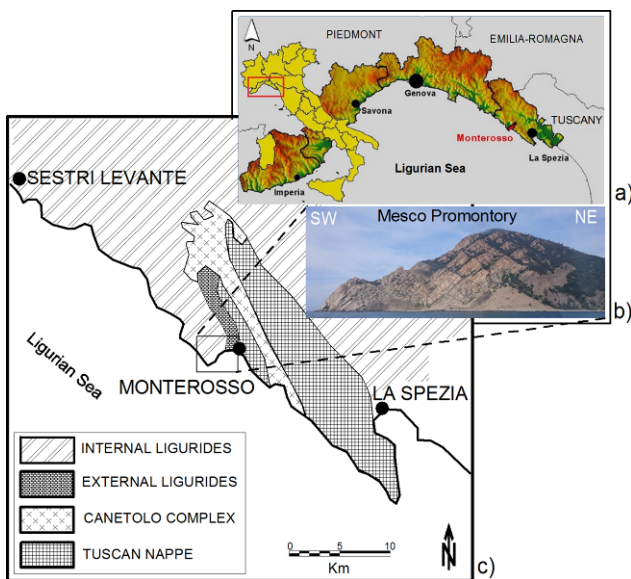


Figure 1. (Color online) Geographical setting (a) and geological sketch (c) of the study area (modified from [13,14]). Panel (b) shows the Mesco Promontory cliff. The Digital Terrain Model (DTM) used in Fig. 1a is modified from [17].

The area of Monterosso is characterized by four overlapping tectonic units (Figure 1c): the Tuscan Nappe, Internal Ligurides Unit, External Ligurides Unit and Canetolo Complex ([10,13,14]). The Tuscan Nappe outcrops on the Western side of Monterosso bay and, in particular, along the thick turbidites of the Macigno Formation (Upper Oligocene). The latter is largely outcropping along most of the Cinque Terre coast. It represents the reverse flank of the west-ward recumbent fold, dipping weakly towards NNW ([15,16]). The Internal Ligurides consist of a Jurassic ophiolite basement

with pelagic cover, followed by a turbidite sequence of Late Cretaceous [9]. This lithological sequence outcrops along the entire NE-SW slope of the Mesco Promontory, which is the target of this study.

3. Structure-from-Motion

Like traditional stereoscopic photogrammetry, SfM provides a 3D photorealistic point cloud or also a 3D photorealistic mesh from a series of overlapping, multi-frame images. The significant advance that characterizes SfM with respect to the other photogrammetric techniques is the automatic alignment of the images in the same reference frame by means of efficient feature-based or area-based matching techniques [18]. A comparative analysis of the performance for several SfM packages, in particular the image alignment, is provided by [19].

In general, targets having known positions and preliminary camera calibration are not strictly necessary. If no external information is used, the obtained model is defined with respect to a non-metric reference frame and, therefore, cannot be really used to quantify changes. In order to obtain a useful model, the scale factor and, if necessary, the data georeferencing must be introduced by means of roto-translation and scaling transformation. Such a transformation can be carried out on the basis of the coordinates of several GCPs. In the cases when camera positions during surveys are known (e.g. if the camera is equipped with GNSS receiver), these data can be used as initial points for the iterations, leading to a considerable reduction of the calculation time and a further increase of the already high chances of success of the alignment process.

It should be noted that, for a digital camera, the focal distance and the internal orientation parameters are normally included in the metadata of the images in any of the known data format (JPEG, TIFF, ...). Nevertheless, models can also be reconstructed from images lacking of metadata, which is the case of images downloaded from the Internet, even if the price to be paid is an increased of both computational effort and probability of incorrect alignment. A reasonable estimate of the final modeling error magnitude is 1:1000, i.e. ± 1 mm error for each 1 m of acquisition distance [20].

This technique is increasingly used and has been successfully applied to geological surveying [6], seismic landform mapping [21] and also architectural survey [22].

The success of a photogrammetric survey mainly depends on [23]: a) good spatial distribution of the camera positions; b) capture of both the whole subject and the detail, preventing occlusions when possible; c) appropriate coverage with wide overlap between images of adjacent areas; e) observation in similar light conditions, therefore preventing shadows and overexposed or underexposed images that could cause the image alignment fail.

The Ground Sampling Distance (GSD), i.e. the distance between the centers of two adjacent pixels measured on the observed object, is a significant parameter in a photogrammetric survey. This parameter expresses the image resolution and therefore constrains the resolution that can be reached in photogrammetric modeling. The GSD is provided by $GSD = p d / f = L_i d / (f N_i)$, where p is the side of the single pixel of the array, d is the

acquisition distance, f is the focal length, L_1 (L_2) is the sensor width (height) and N_1 (N_2) is the number of pixels in width (height). The parameters provided by the camera manufacturer are f , L_1 , L_2 , N_1 and N_2 . A photogrammetric survey must be planned on the basis of the required model resolution and, therefore, of the required GSD (choice of camera and VPs), according to the recommendation a). It should be noted that GSD is not necessarily the resolution of the final 3D object (point cloud or model), but it a limit for such a resolution, as discussed in Section 6.

4. Surveys and Data Processing

4.1. Surveys

Four photogrammetric surveys, called SM1, SM2, SD1 and SD2 respectively, were carried out in April/May 2015 (in the next sections, the point clouds and models are labeled as the corresponding surveys). The aim of the surveys was to extract a digital model of the observed land surface to characterize the geomorphological features of the investigated area.

The images were collected by means of three high resolution cameras: Nikon D750 (surveys SM1 and SM2), Sony Nex7 (SD3) and GoPro Hero3 (SD4). The main technical specification are summarized in Table 1. Figure 2 shows the map of GSD vs. acquisition distance for the three cameras. This figure highlights that the best resolution is obtained by Nikon D750 camera (~2 cm GSD at 150 m).

Table 1. Camera Technical specifications.

Camera feature	Camera Model		
	Nikon D750	Sony Nex7	GoPro Hero3
Sensor size (mm)	35.4 x 24	23.5 x 15.6	5.8 x 4.3
Sensor pixels (px)	6016 x 4016	6000 x 4000	4000 x 3000
Pixel number (Mpx)	24.2	24	12
Depth (bit)	24	24	24
Focal length (mm)	50	16	3
35 mm equivalent focal length (mm)	50	24	17
f-number (f)	f/9	f/6.3	f/2.8
Shutter speed (s)	1/800	1/250	1/701
Sensibility (ISO)	320	100	100
File format	jpeg	jpeg	jpeg

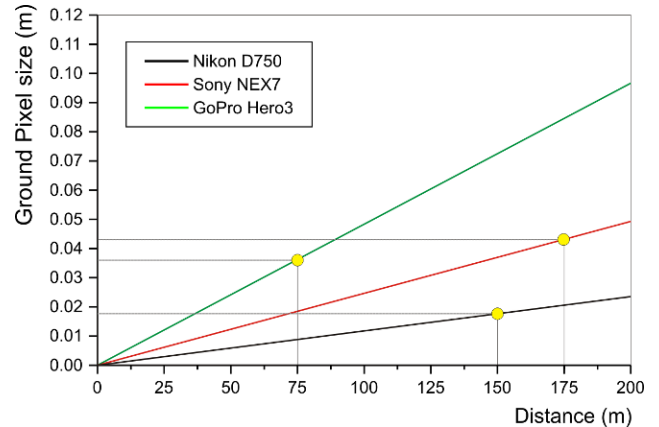


Figure 2. (Color online) Map of GSD vs. acquisition distance for the used cameras. Yellow circles indicate the mean acquisition distance for each camera

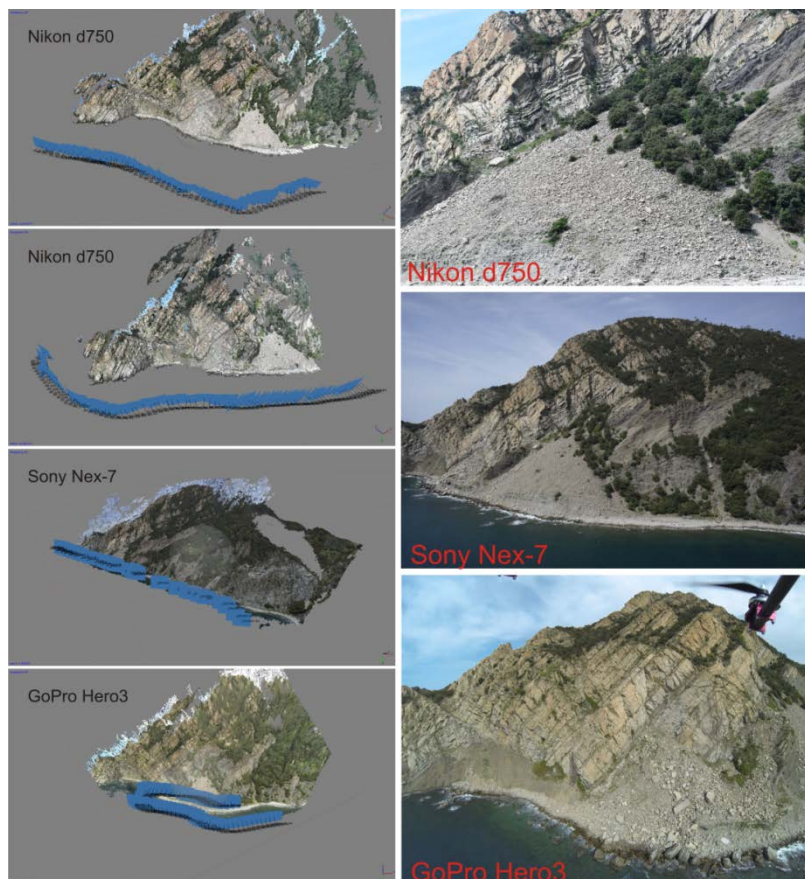


Figure 3. (Color online) Left panels: camera position and orientation during the surveys. Right panels: three images captured by: Nikon D750, Sony Nex7 and GoPro Hero 3, respectively

The first and second surveys (SM1 and SM2) were carried out on April 29, 2015. In both the cases, the operators moved along the coast using a small boat at a ~150 m mean distance from the shoreline. The images were taken by means of the Nikon D750 camera, capturing 60 and 70 images for SM1 and SM2 surveys respectively, with similar geometrical settings.

The third survey (SD3) was performed on May 6, 2015 by using a UAV controlled by a licensed professional pilot. The Sony Nex7 camera, mounted on the octocopter DJI S1000 equipped with Gimbal head, collected 35 images from ~175 m mean elevation, covering the same areas observed in previous campaigns, but from very different VPs; in this case, the photos were taken from about zenithal directions. The VPs were better distributed around the coastal area because the camera occupied 3D positions, therefore not limited to the sea surface. Finally,

an additional aerial survey (SD4) was performed on May 6, 2015, using a home-made quadcopter UAV, equipped with a GoPro Hero3 camera. In this case, 64 low resolution images were collected from an average elevation of ~75 m. Fig. 3 shows the camera positions for the four considered campaigns as well as three examples of photos taken with different cameras and, therefore, characterized by different quality.

4.2. Data Processing

Each data set acquired in the previously described surveys was processed by means of the Agisoft PhotoScan software package [24], which is especially conceived for SfM-based processing of digital images and 3D spatial data generation.

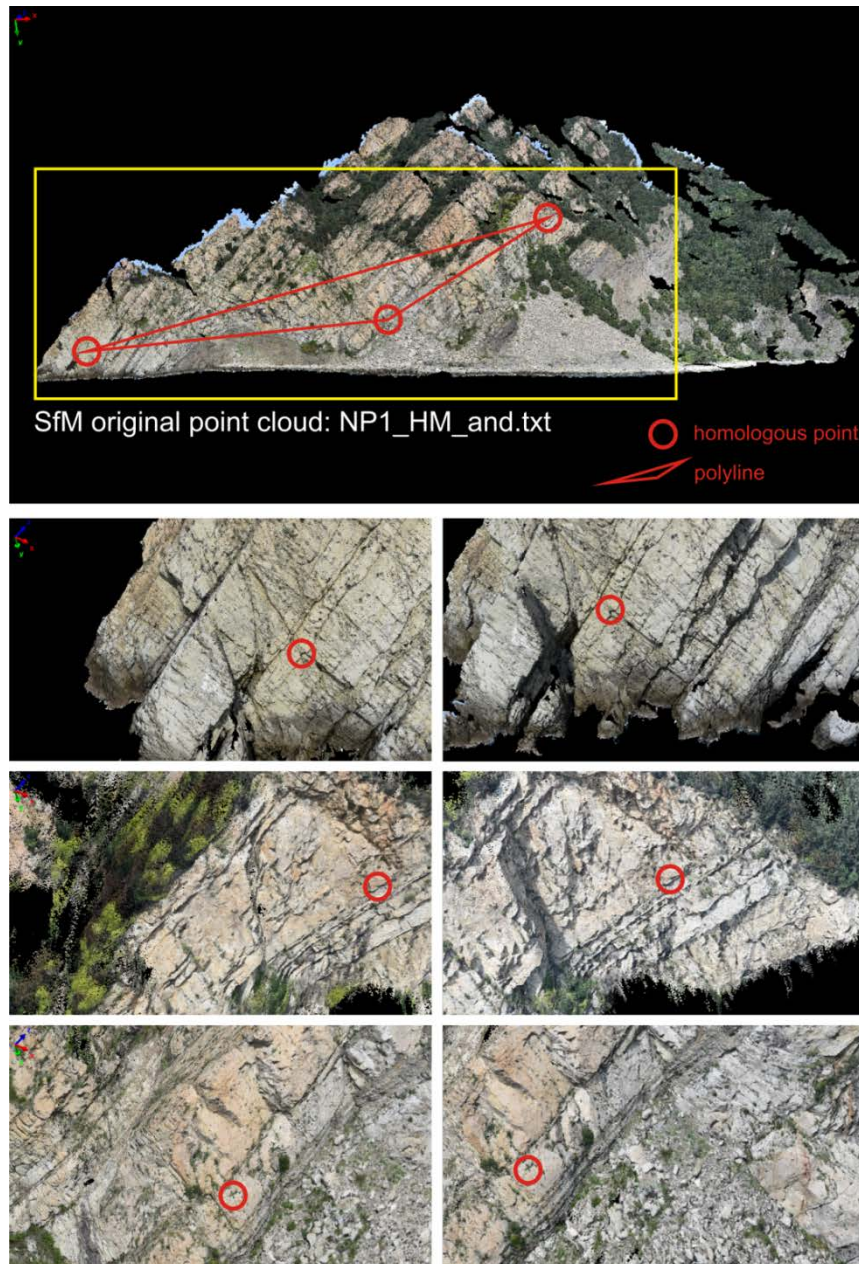


Figure 4. (Color online) Detection of homologous points and creation of the closed polyline for perimeter length computation on a point cloud. The metrical scale is not yet defined and, therefore, is not shown here

In general, four options are possible for SfM data processing:

- (1) Free-net Bundle Adjustment (BA) modeling, where the point cloud is generated in an entirely

automatic way by direct use of the available images, without any constraint about GCPs and/or camera position. In this way, a point cloud defined with respect to a non-metric reference frame is obtained. In particular, a scale factor must be introduced in order to obtain a metric point cloud.

- (2) Use of several GCPs well distributed on the investigated area and whose positions are measured by means of GNSS receivers, total station or other topographical techniques. Two sub-options are possible:
 - (2a) Georeferencing by attribution of the coordinates of at least three GCPs with respect to an external, absolute reference frame to the corresponding points recognized in the free-net BA and computation of the global affine transformation (clearly, if more than three GCPs are assigned, a least square approach is used);
 - (2b) Georeferencing by incorporating the GCPs into the BA model. Such an approach provide the better results thanks to an optimization of the registration at both local and global scale, with errors than can be better by an order of magnitude with respect to the (2a) case.
- (3) Introduction of coordinates for some camera positions, incorporated into the BA model. In this case, the alignment is optimized on the basis of the known positions (that could be a fraction of the whole set of images). For example, camera positions with ~5-10 cm accuracy can be measured if a UAV equipped with a compact Inertial Measurement Unit (IMU) is used. An IMU is very expensive (typically 30,000-40,000 €). A similar accuracy can be achieved if a UAV equipped with a less expensive dual antenna GNSS receiver is used and differential measurements with respect to a base station are carried out [25]. Even better results can be obtained if the used UAV is equipped with both IMU and GNSS receiver.
- (4) A combination of options (2) and (3), in particular (2b) and (3).

All these options are available in PhotoScan. Surely, the option (2b), or a combination of (2b) and (3), provides the better results, leading to a georeferenced point cloud having the correct scale and characterized by alignment residuals particularly low. Nevertheless, GCPs must be adequately distributed on the observed surface, and this is sometimes vary hard or also impossible.

In the specific case, all the surveys were carried out without use of GCPs or UAV equipped with IMU because the aim of this study was to obtain a DSM, a DTM or at least an accurate point cloud in emergency conditions, where GCPs cannot be placed on a cliff and a UAV with IMU could be unavailable because of its high cost. Therefore, SfM data processing provided point clouds originally defined into a local reference system less than a scale factor, i.e. a free-net BA modeling was carried out.

The proposed strategy for the registration of the whole coordinates data set into an external reference frame, therefore solving the problem of scale factor, was based on few simple steps: (i) a point cloud was chosen as reference set of coordinates; (ii) some points, related to well recognizable features, were recognized in each point cloud; (iii) for each point cloud, the selected points were pairwise connected leading to a closed poly-line whose perimeter was calculated; (iv) the ratio between the perimeter lengths with respect to the reference one provided the relative scale factor to resize all the point clouds to the scale factor of the reference point cloud; (v) the point clouds were aligned on the reference one by estimating the best parameters for a rigid transformation (i.e. a roto-translation) in a least square approach; (vi) a final and unique transformation was applied to the whole data set by using an external model as new reference and repeating the operational procedure described in (i)-(v). This method is designed to optimize the results in terms of scaling and aligning of point clouds obtained from SfM. Following this procedure the internal differences between the SfM models are supposed to be minimized and a possible error of registration into an external reference frame (which can be georeferenced) is common to all of the point clouds. It is important to point out that the approach is conceived for a fast data processing and a preliminary evaluation of the results if GCPs are unavailable.

In the specific case, the point cloud obtained by SfM-based processing of images from the first survey (SM1) was used as reference. The operations (i)-(vi) were carried out by using the PolyWorks software package [26]. The large amount of features recognizable on the point clouds allowed an easy recognition of the homologous points for the polyline generation.

Figure 4 shows the procedure applied to point clouds SM1 and SM2. In order to have closed polylines and compute a scale factor representative of the entire zone, at least three homologous points well distributed on the observed surface must be selected. It should be noted that these points are not directly used to carry out similarity transformations; the polyline lengths are used instead. Moreover, the perimeter length was computed several times to create a reasonable statistics and to calculate the mean of measurement as the more realistic value.

Table 2. Closed polyline lengths and relative and absolute scale factors. Note that the units u1-u4 are dimensionally lengths.

Survey	SM1	SM2	SD3	SD4	UTM
	(u1)	(u2)	(u3)	(u4)	(m)
Perimeter	48.4015	49.1185	27.1626	60.0428	909.72
SD	0.0006	0.0005	0.0004	0.0005	0.06
Scale factors (%)					
Relative %	100	98.5	178.2	80.6	-
UTM %	1879.5				

Table 2 lists the means and the standard deviations for perimeters extract from the four point clouds together with the relative scale factor applied to the point clouds SM2, SD1 and SD2. The point clouds were aligned on the reference one in a standard way, i.e. by means of Iterative Closest Point (ICP) algorithms implemented in PolyWorks software. Finally, using external data extracted from a previous model based on Terrestrial Laser Scanning (TLS) measurements, a common transformation

was applied to the whole SfM data set of point clouds leading to four complete models of studied areas defined with respect to the WGS84/UTM 32N coordinate system.

5. Results

This section shows the results of the comparison between point clouds in order to highlight significant differences. In order to provide significant and interpretable results, two very different areas were selected: an area represented by solid and stratified rocks (A in Figure 5) and an area characterized by the presence of a deposit of incoherent material (B).

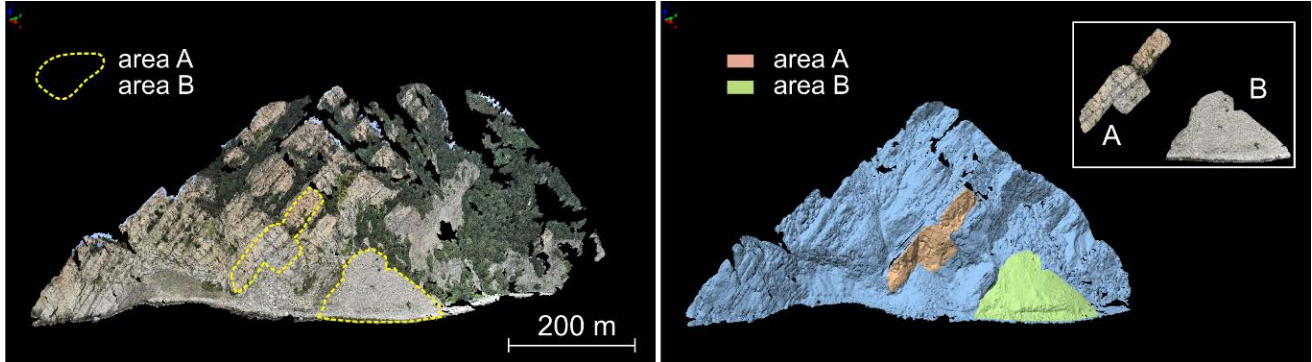


Figure 5. (Color online) Selected sample areas (A and B). Left: SM1 point cloud; right: corresponding digital model

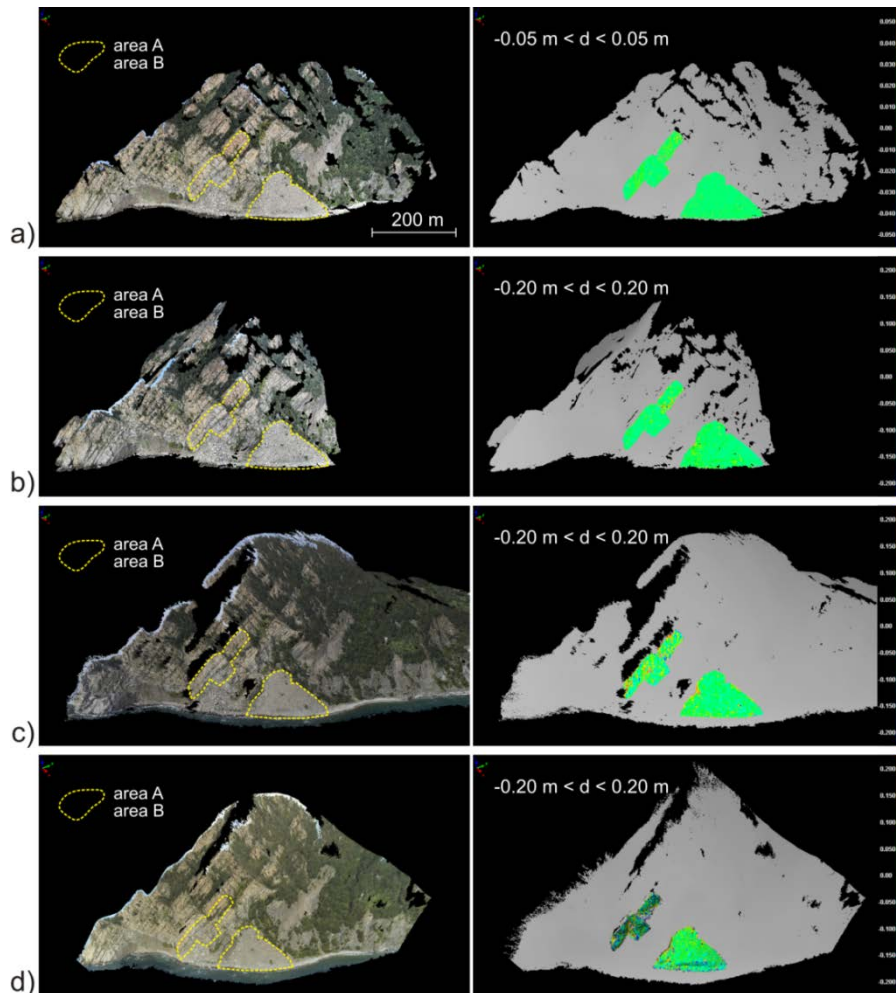


Figure 6. (Color online) Point clouds and differences maps. a) SM1 point cloud to SM1 model; b) SM2 point cloud to SM1 model; c) SD3 point cloud to SM1 model; d) SD4 point cloud to SM1 model

It should be noted that PolyWorks allows the computation of differences between point clouds throughout an intermediate step, i.e. the creation of a digital model from the reference point cloud (the model is defined on a regular grid parallel to the point cloud, i.e. is 2.5D model) and subsequent point-to-surface distance computation. The differences are recursively computed for

all the elements of the second point cloud along the normal directions of areal elements of the reference model. For this reason, a qualitative and quantitative estimation of internal model errors are also provided, i.e. the comparison between the point cloud SM1 and the corresponding 2.5D model is also considered here.

Table 3. Main results of comparison between the point clouds and the model SM1. For each case and each component, mean (μ) and standard deviation (σ) of differences are shown for the two selected areas A and B.

Case		dx (m)		dy (m)		dz (m)	
model	Point cloud	μ	σ	μ	σ	μ	Σ
SM1	SM1_A	0.00	0.01	0.00	0.01	0.00	0.01
SM1	SM1_B	0.00	0.01	0.00	0.02	0.00	0.01
SM1	SM2_A	0.00	0.04	0.00	0.03	0.00	0.05
SM1	SM2_B	0.01	0.07	0.00	0.05	0.00	0.05
SM1	SD3_A	-0.01	0.06	0.01	0.05	-0.01	0.09
SM1	SD3_B	-0.02	0.15	0.03	0.16	-0.02	0.14
SM1	SD4_A	-0.00	0.05	-0.00	0.04	0.01	0.08
SM1	SD4_B	0.02	0.15	0.02	0.13	0.01	0.11

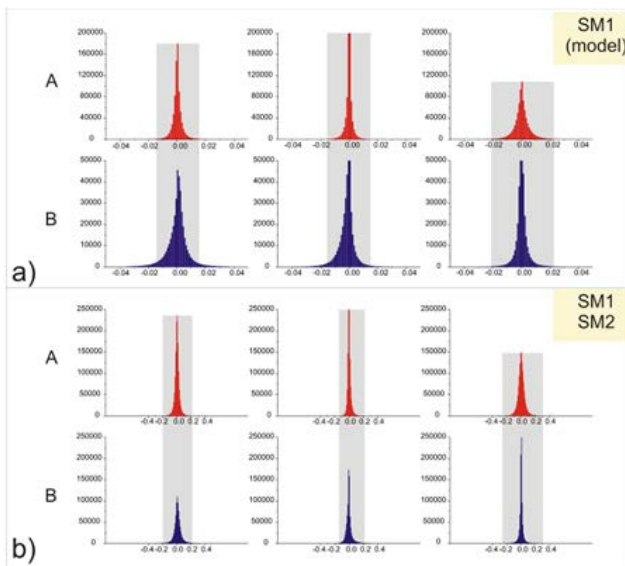


Figure 7. (Color online) a) Distributions of differences between the point cloud SM1 and the digital model obtained from SM1; b) Distributions of difference between the point cloud SM2 and the digital model from SM1. Top panels: A-area; bottom panel: B-area. From left to right: x, y and z component.

Figure 6 shows the maps of differences obtained by comparing all the four point clouds to the reference model from SM1. For each point cloud, the points belonging to the selected areas A and B are extracted and analyzed leading to mean, Standard Deviation (SD) and frequencies of the corresponding distributions for the x, y and z coordinates (Table 3, Figure 7). In particular, Figure 7a shows the distributions of the residuals between the point cloud SM1 and the corresponding model. The mean is ~ 0 cm and the SD 1 cm for all the components in A-area and never exceeds 2 cm for all the components in B-area (Table 3). These results and fact that the SDs in all the other cases are significantly greater (range: 4-16 cm) imply that the errors due to comparison with respect to the digital model can be neglected.

In order to summarize the results of statistical analyses, a synthetic graph is proposed, showing means and SDs for all the considered comparisons with respect to the model related to SM1 (Figure 8). The main results that emerges from this analysis are that the point clouds are characterized by high repeatability and the averages of differences are centered around the zero value, taking into account the corresponding standard deviations. Moreover, this graph highlights that SDs related to B-zone

(incoherent material) always are greater than those relative to A-zone (stratified rock).

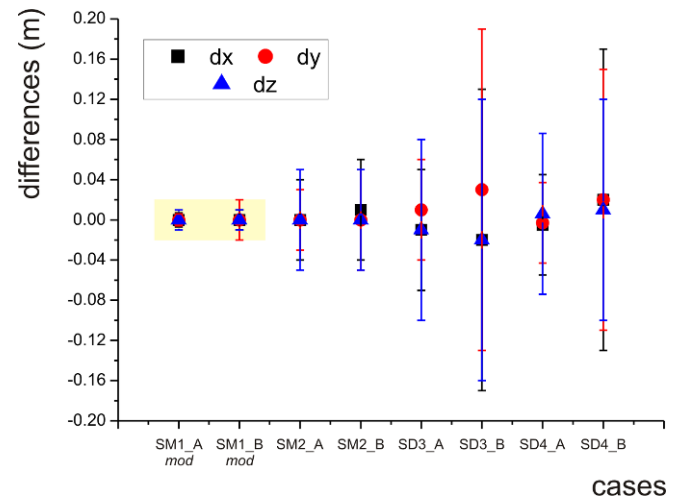


Figure 8. (Color online) Mean and standard deviation for the considered comparisons with respect to the model from SM1 survey. The same result is zoomed in the left part of the figure

6. Discussion and Conclusions

The results show that SfM technique can provide high resolution photorealistic point clouds and DSMs through simple and fast image acquisition. In particular, if the surveys are well planned and carried out, good results can be obtained without use of GCPs. It is important to highlight that this study is aimed at evaluating the kind and quality of the information that can be obtained by fast digital photogrammetry surveys, in particular in emergency conditions.

The point clouds provided by boat-based near offshore surveys are characterized by the better resolution because of a better compromise between camera quality (Nikon D750, surveys SM1 and SM2) and acquisition distance (~ 150 m), i.e. lower GSD (~ 2 cm; Figure 2).. However, despite the worse GSD (~ 4.5 cm survey SD3, with Sony Nex7; ~ 3.5 cm survey SD4, camera GoPro Hero3), results from UAV-based surveys are close to those from boat-based ones. This is due to a better acquisition geometry that can potentially provide a more robust framework of the whole observed system. The GSD is related to the final resolution of the provided point cloud and/or 3D digital model, and in particular is a limit for the model resolution. Anyway, two other important factors impact on the point cloud quality: the camera positions and the density of point cloud chosen in the SfM-based image processing phase. The first requires a good survey planning. In the specific case of Cinque Terre surveys, the near offshore boat-based image acquisition allowed a good cover of the lower zone of the observed area thanks to a good VP distribution in 2D, but the model of the upper part was partially incomplete and had at lower quality because the camera position was just about 2 m above the sea level. Conversely, the UAV-based surveys fully covered the studied area. The second factor is strictly related to the available hardware resources because the SfM computations require significant processing power and several hours of calculations are necessary.

In general, the obtained results highlight the importance of the use of a large quantity of overlapping images. As a boat navigates or a UAV flights, images must be continuously acquired. It must be noted that a large number of redundant images must be taken. This is not a problem with modern cameras and memory cards. Moreover, if an overabundant image set is available, some SfM data processing packages (e.g. PhotoScan) allow an automatic extraction of the subset of images whose photogrammetric processing leads to the best results.

The comparisons between the point clouds carried out in two sample areas (A: stratified rock; B: incoherent material) show that no significant differences appear in the case of the rock cliff, whereas significant differences may occur between the point clouds that represent the incoherent material. This effect can be related to a slight VP change in the B-area that can lead to significant differences in SfM-based modeling because of local complexity of such a strongly irregular system. A complete and accurate modeling of an incoherent material area, aimed e.g. at performing volumetric measurements, requires a large amount of images.

Although the results suggest that a UAV is the better platform for a SfM survey, in a coastal area a boat could be the only available platform for a fast survey in emergency conditions. The current aerial navigation rules restrict the use of a UAV in inhabited areas and, in addition, each combination UAV/payload must be certified in Italy by ENAC (Italian Civil Aviation Authority). Even if some rules can be attenuated in emergency conditions, in normal use a UAV survey could not be performed in a short time. The results show that a boat-based survey can easily be used to quickly characterize a coastal area if a camera with high resolution sensor and high quality lens is used from a reasonable distance and with a good spatial distribution of VPs. These results also suggest the planning of an experiment aimed at finding a simple and direct relation between the technical specifications of the available cameras and the achievable model resolution and precision as a function of the maximum elevation of the camera VPs. In other words, the effects of 3D and 2D spatial distributions of camera VPs on the quality of the final point cloud/3D model should be explored.

In the specific case, the problem of the model scale factor was solved by selection, on each SfM-based point cloud and on the available georeferenced point cloud provided by a TLS survey, of several points related to some recognizable features and subsequent generation of the polyline linking these points. This fact is not in contradiction with the character of the survey and data processing (i.e. fast and cheap). This because, if a reference model is unavailable, the same results can be obtained by means of a Total Topographical Station (TTS) that can acquire the features recognized on the SfM-based point clouds. If a reflectorless TTS is used, no contact with the studied system is required. If TTS data are unavailable, the coordinates of some reference points can be recognized in Google Maps/Google Earth aerial photos, leading to a reference polyline. In this way, a raw scale factor can be obtained. Although it should be affected by ~1-2% uncertainty, it could be used for an initial evaluation of survey results in emergency conditions.

The used approach corresponds to a free-net BA with subsequent data georeferencing. Therefore, good results can be obtained if the studied system has a size not higher than 2-3 km, typical for surface-based or UAV-based surveys. If larger systems must be studied, in order to keep the errors within reasonable thresholds, the GCP data should be preferably integrated into the BA modeling [27].

In conclusion, the SfM technique allows a fast and easy acquisition and modeling of a natural surface like a sea cliff, without the use of GCPs, and is compatible with an observation carried out from a floating platform, leading to point clouds having a resolution of a few centimeters for an acquisition distance of 100-150 m.

Acknowledgment

The research activities were carried out within the framework of the SCANCOAST Project, funded by Regione Liguria, Regional Operational Plan (2007-2013) Axis 1 DLTM (Distretto Ligure delle Tecnologie Marine).

Competing Interests

The authors have no competing interests.

List of Abbreviations

GCP	: Ground Control Point;
GSD	: Ground Sampling Distance;
GNSS	: Global Navigation Satellite System;
DSM	: Digital Surface Model;
DTM	: Digital Terrain Model;
IMU	: Inertial Measurement Unit;
SfM	: Structure-from-Motion photogrammetry;
TLS	: Terrestrial Laser Scanning;
TTS	: Total Topographical Station;
UAV	: Unmanned Aerial Vehicle;
VP	: Viewpoint.

References

- [1] Z. Li, Q. Zhu and C. Gold, Digital Terrain Modeling. Principles and methodology, CRC press, Boca Raton FL, 2005.
- [2] Anzidei, M., Esposito, A., Bortoluzzi, G. and De Giosa, F., "High resolution Bathymetric map of the exhalative area of Panarea (Aeolian Islands, Italy)," *Annals of Geophysics*, 48 (6). 899-921. Dec.2005.
- [3] Delacourt, C., Allemand, P., Berthier, E., Raucoules, D., Casson, B., Grandjean, P., Pambrun, C. and Varel, E., "Remote-sensing techniques for analysing landslide kinematics: a review," *Bulletin de la Société Géologique de France*, 178 (2). 89-100. 2007.
- [4] Travalletti, J., Malet, J.-P. and Delacourt, C., "Image-based correlation of Laser Scanning point cloud time series for landslide monitoring," *International Journal of Applied Earth Observation and Geoinformation*, 32. 1-18. Oct.2014.
- [5] Benoit, L., Briole, P., Martin, C., Tom, C., Malet, J.-P., and Ulrich, P., "Monitoring landslide displacements with the Geocube wireless network of low-cost GPS," *Engineering Geology*, 195. 11-121. Sep.2015.
- [6] Westoby, M.J., Brasington, J., Glasser, N.F., Hambrey, M.J. and Reynolds, J.M. "'Structure-from-Motion' photogrammetry: A low-cost, effective tool for geoscience applications," *Geomorphology*, 179. 300-314. Dec.2012.

- [7] Tarolli, P., Preti F. and Romano, N., "Terraced landscapes: From an old best practice to a potential hazard for soil degradation due to land abandonment," *Anthropocene*, 6. 10-25. Jun.2014.
- [8] Abbate E., Bortolotti, V., Passerini, P., and Sagri, M., "The Northern Apennines geosyncline and continental drift," *Sedimentary Geology*, 4 (3-4). 637-642. 1970.
- [9] Marroni, M., Monechi, S., Perilli, N., Principi, G. and Treves, B., "Late Cretaceous flysch deposits of the Northern Apennines, Italy: age of incision of orogenesis-controlled sedimentation," *Cretaceous Research*, 13. 487-504. Sep.1992.
- [10] Bortolotti, V., Principi, G. and B. Treves, B., *Ophiolites, Ligurides and the tectonic evolution from spreading to convergence of a Mesozoic Western Tethys segment*, in *Anatomy of an Orogen: the Apennines and Adjacent Mediterranean Basins*, Kluwer Academic Publishers, Dordrecht, the Netherlands, 2001, 151-164.
- [11] Bernini, M. and G. Papani, G., "La distensione della fossa della Lunigiana nord-occidentale," *Bollettino della Società Geologica Italiana* 121 (3). 313-341. Oct.2002.
- [12] Ferranti, L., Antonioli, F., Anzidei, M., Monaco, C. and P. Stocchi, P., "The timescale and spatial extent of vertical tectonic motions in Italy: insights from relative sea-level changes studies," *Journal of the Virtual Explorer*, 36 (30).
- [13] Cerrina Feroni A., Martinelli, P. and Ottria, G., "La posizione dei Flysch ad Elmintoidi (Formazione del M.te Antola e di Ortonovo) nella piega Castelpoggio-Ortonovo a NW delle Alpi Apuane," *Accademia Nazionale delle Scienze detta dei XL, scritti e documenti*, 14. 181-193. Jun.1995.
- [14] ISPRA - Servizio Geologico d'Italia, "Carta Geologica d'Italia in scala 1 :50.000 - Foglio n. 247," Levante, Roma, 2011.
- [15] Giammarino, S. and Giglia, G., "Gli elementi strutturali della piega di La Spezia nel contesto geodinamico dell'Appennino Settentrionale," *Bollettino della Società Geologica Italiana*, 109 (4). 683-692. Nov.1993
- [16] Cevasco, A., "I fenomeni di instabilità nell'evoluzione della costa alta delle Cinque Terre (Liguria Orientale)," *Studi Costieri*, 13. 93-109. 2007.
- [17] Bisson, M., Fornaciai, A., and F. Mazzarini, F., "A geographic database used for GIS applications," *SITOGEO*, 30 (3), 325-335. May.2007.
- [18] Granshaw, S.I., and Fraser, C.S., "Editorial: Computer Vision and Photogrammetry: Interaction or Introspection?," *The Photogrammetric Record*, 30 (149). 3-7. Mar.2015
- [19] Remondino F, Spera, M.G., Nocerino, E., Menna, F. and F. Nex, F., "State of the art in high density image matching," *The Photogrammetric Record*, 29 (146), 144-166. Jun.2014.
- [20] James, M.R., and Robson, S., "Straightforward reconstruction of 3D surfaces and topography with a camera: Accuracy and geoscience application," *Journal of Geophysical Research*, 117 (F03017).
- [21] Ninfo, A., Zizioli, D., Meisina, C., Castaldini, D., Zucca, F., Luzi, L., and De Amicis, M., "The survey and mapping of sand-boil landforms related to the Emilia 2012 earthquakes: Preliminary results," *Annals of Geophysics*, 55 (4). 727-733. Apr.2012.
- [22] Teza, G., Pesci, A. and Ninfo, A., "Morphological analysis for architectural applications: comparison between laser scanning and Structure-from-Motion photogrammetry," *Journal of Survey Engineering*, Jan.2016.
- [23] N. Micheletti, J.H. Chandler, and S.N. Lane, *Structure from Motion (SfM) photogrammetry*, in *Geomorphological Techniques*, British Society of Geomorphology, London, 2015. [E-book] Available: http://www.geomorphology.org.uk/sites/default/files/geom_tech_chapters/2.2.2_sfm.pdf. [Accessed March 3, 2016].
- [24] Agisoft PhotoScan web site. Available: <http://www.agisoft.com>. [Accessed March 3, 2016].
- [25] Barry P. and Coakley, R., "RPAS photogrammetry," *Civil Engineering Surveyor*, 2013(07/08). 37-41. Jul.Aug. 2013.
- [26] Innovmetric PolyWorks software package web site. Available: <http://www.innovmetric.com>. [Accessed March 3, 2016].
- [27] Sun Y., Zhao, L., Zhou, G. and Yan, L., "Absolute Orientation Based on Distance Kernel Functions," *Remote Sensing*, 8 (3). 213-231. Mar.2016.